JOURNAL OF GEOPHYSICAL RESEARCH, VOL. 111, F04008, doi:10.1029/2005JF000403, 2006

Fracture toughness of dry snow slab avalanches from field measurements

D. M. McClung[1] and Jürg Schweizer[2]

Received 13 September 2005; revised 1 March 2006; accepted 15 May 2006; published 25 November 2006.

[1] Dry snow slab avalanches release by propagating fractures. The first fracture occurs in shear within a thin weak layer underneath a planar slab which eventually fails in tension perpendicular to the weak layer at some distance up-slope. Thus fracture properties of both the weak layer (in shear) and the slab (in tension) are important for determining the character of the slab avalanche including its volume and, hence, destructive potential. In this paper, the fundamental fracture properties relevant during slab avalanche release are evaluated for both weak layer shear and slab tensile fracture from field measurements. Data from nearly 300 slab avalanches are used to estimate tensile and shear fracture toughness. Two important practical results come from the analysis. The first is that, on average, slab tensile toughness is about 5–7 times the weak layer shear toughness with a range of about 2–15. This is of immense practical importance since it allows estimates of slab dimensions (length) and width from measured estimates of the slab depth, D. The second important result is that a length scale is provided for a highly stressed (tensile stress) boundary layer of about 20 cm from the weak layer up through the body of the slab over which the tensile crack should first form. This estimate gives an important scale for field evaluation of snow slab instability for measurements from snow profiles. For example, it gives a guideline for estimating important hardness changes between the weak layer and the slab which have been shown from field data to be associated with human triggering of snow slabs. We expect that our results will provide a framework for analysis of rock avalanches and flake-type landslides which fail on weak interfaces under slabs.

Citation: McClung, D. M., and J. Schweizer (2006), Fracture toughness of dry snow slab avalanches from field measurements, *J. Geophys. Res.*, *111*, F04008, doi:10.1029/2005JF000403.

1. Introduction

[2] Direct visual observations and measurements of dry slab avalanches show that they result from an initial shear fracture in a weak layer underneath a slab which propagates rapidly up-slope and across-slope until tensile fracture occurs through the body of the slab [*McClung*, 1979, 1981]. Within the realm of natural fracture propagation in nature, direct human experience with release of snow slabs probably exceeds that of any other type of fracture. In North America and Europe, more than 90% of victims trigger the slabs themselves [*McClung and Schaerer*, 1993], and there are countless field observations in regard to fracture initiation and propagation. In situ strength and hardness indices of slab and weak layer properties show that the slab has higher strength than the weak layer. Furthermore, there are persistent observations that harder, higher-strength slabs (called hard slabs) give rise to larger slab volumes than less strong ones (called soft slabs), and slab dimensions (length and width) increase with slab thickness D. These observations and measurements suggest that slab hardness, or tensile strength, is important for determining slab volume and, hence, destructive potential. Further, they suggest that initial snow slab instability is controlled by shear fracture toughness in the weak layer [*Bažant et al.*, 2003b; *McClung*, 2005a] while snow slab size may be controlled by slab tensile fracture toughness. Since both the shear and tension failures are generated by propagating fractures, it is expected that fracture toughness rather than strength is of fundamental importance [*Bažant et al.*, 2003b; *McClung*, 2005a] since the concept of strength has no meaning by itself in fracture initiation and growth.

[3] Alpine snow is a quasi-brittle material from the perspective of fracture initiation processes. It is expected that snow strain-softens at any rate [*Bažant et al.*, 2003b] in either shear [*McClung*, 1977] or tension [*Narita*, 1980, 1983; *Sigrist et al.*, 2005] prior to fracture, and the grain size is in the range of millimetres. These characteristics imply that for fracture the fracture process zone (FPZ) containing the region where failure is taking place is of relatively large size, i.e., at least a significant fraction of

[1] Department of Geography, University of British Columbia, Vancouver, British Columbia, Canada.
[2] Swiss Federal Institute for Snow and Avalanche Research, Swiss Federal Institute for Forest, Snow and Landscape Research (WSL), Davos, Switzerland.

0148-0227/06/2005JF000403$09.00

snow slab thickness D [*Bažant et al.*, 2003b; *McClung*, 2005a]. The quasi-brittle character means that the classical Griffith theory of brittle fracture developed during the 1920s [*Griffith*, 1921, 1924] will not apply to alpine snow and snow avalanche initiation since a fundamental assumption is an infinitesimal FPZ. Further, it implies a fracture mechanical size effect in either tension or shear: Strength decreases as characteristic size, D, increases.

[4] *Bažant et al.* [2003b] provided the size effect law for the snow slab for weak, layer fracture in shear (mode II). *McClung* [2005a] estimated shear fracture properties including shear fracture toughness, $K_{IIc}(D)$ from fracture line data for hundreds of snow slabs.

[5] The aim of this paper, is to provide a companion size effect law appropriate for slab tensile fracture toughness $K_{Ic}(D)$ (mode I fracture toughness) and to provide estimates of slab tensile fracture toughness and other fracture properties from field data for hundreds of snow slabs. By applying concepts from both the shear and tensile size effect laws, we are then able to estimate the approximate ratio of tensile to shear fracture toughness.

[6] Two results of immense importance arise from our analysis. First, the ratio of slab tensile toughness to shear fracture toughness enables estimates of slab dimensions (length and width) given the depth. Derivation of these values requires dynamics fracture mechanics and is beyond the scope of the present paper, but it is planned for a forthcoming companion paper on the basis of the results here. The second important result is that a length scale of about 20 cm is provided for a highly stressed boundary layer at the bottom of the slab. We suggest that the tensile crack which finally brings down the slab is formed in this region. The importance of estimating the change in properties, for example hand hardness, between the weak layer and the slab has been noted from empirical studies of slab release associated with human triggering [*McCammon and Schweizer*, 2002] but our paper provides the first quantitative estimate as a guide for application of field measurements to evaluate snow instability.

[7] The results suggest that, on average, slab tensile fracture toughness is about 5 times weak layer shear fracture toughness. Since the results are derived from field measurements, the precision expected from laboratory experiments cannot be achieved. However, the results are encouraging in that expectations from field observations and measurements are matched: Slab toughness should exceed weak layer toughness, and there should be substantial variations as implied by the analysis. The advantage of using hundreds of large, full-scale samples (actual avalanches) may outweigh the lack of precision and the difficulty of extrapolating small lab samples to the problem. We suggest that our results give information of fundamental importance for snow slab instability, estimation of slab dimensions and expected destructive potential related to avalanche size.

[8] The problem of a stiff slab overlying a weak layer is not unique to snow avalanches in geophysics. We suggest our results will have application in some cases to rock avalanches and flake-type landslides for which a weak layer or interface can be identified. The historic paper on the subject for landslide initiation and progressive failure by *Palmer and Rice* [1973] was published more than 30 years ago but geoscientists have been slow to grasp the significance of the fracture mechanical approach. We believe that a quasi-brittle fracture mechanical approach has a much more realistic physical basis for this class of problems than the classical factor of safety: ratio of shear strength to shear stress which ignores important size effects and fracture properties. For slope failures which involve fracture and strain softening, the concept of shear strength has no meaning by itself [*Bažant et al.*, 2003b], and the important applications such as estimates of slab dimensions which follow from energy concepts, as implied for fracture, will not evolve if strength is used alone in a stability condition based only on a stress condition with size effects ignored.

2. Dry Slab Avalanche Release

[9] Field observations show that the fracture sequence for the dry snow slab is (1) up-slope (mode II) and cross-slope (mode III) shear fracture; and (2) tensile fracture (mode I) through the crown of the slab. The crown fracture is perpendicular to the bed surface formed by the propagating shear fractures [*Perla*, 1971; *McClung*, 1981, 2005a]. We suggest the tensile fracture most likely initiates at the bottom of the slab [*McClung*, 1981] since dynamic tensile stresses will be highest there. The perpendicular fracture line suggests that propagating shear fractures reduce bed friction to a small value with dynamic stress reorientation so that maximum principal (tensile) stress is oriented parallel to the bed. *McClung* [1981] suggested that a combination of dynamic effects and slab- weak layer orthotropy both contribute to the bed perpendicular fracture line. The thin weak layer under the slab is what makes mode II and mode III propagation possible underneath the slab. Mode II and mode III fracture is not possible in homogeneous snow slabs [*McClung*, 2005a]. For the dynamic problem just described, the tensile stress distribution within the slab should be very complex and nearly impossible to calculate in a real situation. However, a simplified version of the problem is given below, based on the simple geometry. The approximations made, along with use of field data, suggest that only rough estimates of fracture toughness are appropriate with considerable uncertainty.

3. Energetic Fracture Mechanical Size Effect Laws for Quasi-Brittle Materials

[10] According to *Bažant* [2004] there are two types of energetic (nonstatistical) fracture mechanical strength size effect laws applicable to quasi-brittle materials for positive geometry. Positive geometry is required for snow slab release [*Bažant et al.*, 2003b]. This implies stable growth of the FPZ until a peak load is achieved, and once peak load is achieved, a crack will grow unstably [*Rice*, 1968]. The two types of energetic size effect laws are derived below according to whether the specimen is unnotched (type 1) or notched (type 2) for application to snow slab release.

3.1. Type 1: Tensile (Mode I) Fracture of the Slab

[11] Type 1 arises if the geometry is such that maximum load, $P_{\max}$, is reached at crack initiation from the fracture process zone (FPZ) at a smooth (unnotched) surface and fracture takes place as soon as the FPZ is fully formed.

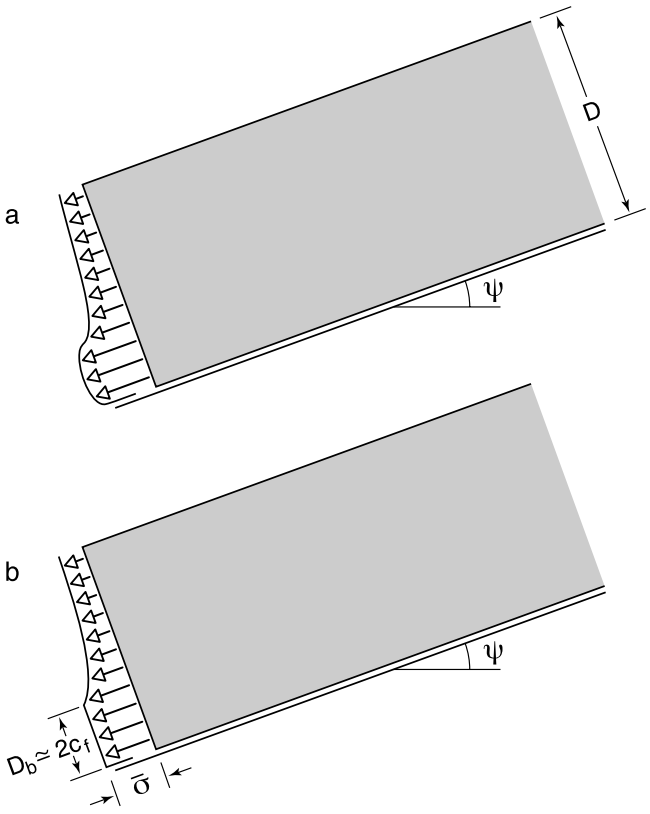

Figure 1. (a) Schematic of tensile strain gradient through a snow slab of thickness D. Tensile stresses are highest at the bottom of the slab. (b) Schematic of approximation for highly stressed boundary layer of thickness $D_b \simeq 2c_f$ with mean tensile stress, $\overline{\sigma}$, in the boundary layer. At failure, $\overline{\sigma}$ is equated to tensile strength, f_t'.

[12] We suggest that a type 1 fracture process and size effect law is appropriate for the tensile (mode I) failure process through the body of the slab. Physically, mode II fracture propagates within the weak layer to build tensile stresses dynamically within the slab [e.g., *McClung*, 2005b]. We suggest, as appropriate for a type 1 law, that a highly stressed boundary layer on the order of the FPZ in thickness appears at the lower boundary of the slab which may be taken to be a smooth surface, unnotched and with positive geometry. When the load reaches $P_{\max}$ and the FPZ is formed, mode I fracture through the slab takes place. *McClung* [1979] provided static stress solutions for strain-softening behavior in shear in a weak layer which suggest a strain and stress gradient in the slab with tensile stresses highest in the region at the base of the slab. Such a strain gradient is a requirement for a type 1 size effect law as there is no size effect under a constant uniaxial state of strain and stress [*Bažant*, 2002]. Figure 1 is a schematic depicting the strain gradient in a snow slab and the approximation of it used in this paper to derive size-scale information about the boundary layer thickness.

3.2. Type 2: Shear (Mode II) Fracture of the Weak Layer

[13] Type 2 occurs if there is a large notch or preexisting crack, and if the geometry is positive. *Bažant et al.* [2003b] and *McClung* [2005a] applied a type 2 energetic fracture mechanical size effect law to the initial shear fracture (mode II) weak layer failure for the snow slab. The preexisting crack in this case is a macroscopic imperfection of the order of at least tens of grain size in length, and the formulation is based on the cohesive crack model introduced originally into landlside slope failure mechanics by *Palmer and Rice* [1973] and applied by *McClung* [1979, 1981] to the snow slab.

[14] In this paper, the concepts are applied consistent with the cohesive crack model in the weak layer using equivalent crack concepts and positive geometry. Observationally, avalanche weak layer shear fracture and slab tensile fractures are characterized by rapid unstable propagation under load after $P_{\max}$ is achieved.

3.3. Mathematical Representations of Energetic Size Effect Laws for Positive Geometry

[15] If σ_N is the average nominal applied tensile stress at failure (replaced by shear stress τ_N for mode II shear fracture), and D is characteristic snow slab thickness, then the following asymptotic limits of the size effect laws apply [*Bažant*, 2002, 2004]:

$$D \to 0 : \sigma_N = b_0 - c_0 D + \ldots \quad \text{(types 1 and 2)} \tag{1}$$

$$D \to \infty : \sigma_N = b_1 + c_1 D^{-1} \quad \text{(type 1)} \tag{2}$$

$$D \to \infty : \sigma_N = D^{-1/2}\left(b_2 - c_2 D^{-1} + \ldots\right) \quad \text{(type 2)} \tag{3}$$

At failure the nominal stresses are replaced by $\sigma_N \to \sigma_{Nu}$; $\tau_N \to \tau_{Nu}$ values of nominal strength. At the lower limit ($D \to 0$) the nominal stress increases to a constant value which is analogous to plasticity failure models: failure at a constant load or stress level with no size effect implied.

[16] At the upper limit ($D \to \infty$), equations (2) and (3) match linear elastic fracture mechanics (LEFM) whereby the FPZ may be considered to be small relative to characteristic slab size D. The intermediate range of sizes between these two limits (10 cm to several meters for the snow slab) is the one of interest for the slab avalanche [*McClung*, 2005a]. The size effect laws used in this paper are gained by asymptotic matching so that at either limit the equations above are obeyed, and reasonable predictions in the intermediate range are expected.

4. Fracture Toughness for a Type 2 Size Effect Law for Slab Failure in Tension From LEFM-Equivalent Crack Concepts

[17] Fracture of a quasi-brittle material in which the fracture process zone is not negligible relative to the dimensions of the specimen is a nonlinear problem. If the fracture process zone extends over a significant portion of the specimen, then complex models are required to represent material behavior in the process zone. However, if a small but nonnegligible portion of the sample is fracturing, then partly linear and simpler models may be used to estimate the response by an equivalent crack far

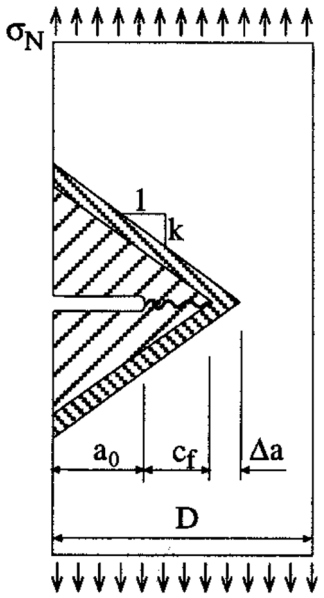

Figure 2. Schematic of the uniaxial stress, σ_N, applied to a notched sample containing a crack with a finite FPZ and the quantities used to derive Bažant's one-dimensional size effect law. Total equivalent crack length is $a_0 + c_f$, k is a material constant, and the FPZ $\approx 2c_f$. From *Bažant and Planas* [1998, p. 14]. Reproduced by permission of Routledge/Taylor and Francis Group, LLC.

from the crack tip by an equivalent elastic crack with the tip somewhere in the fracture zone. For large, but not infinitely large, specimens the true fracture toughness in the equivalent crack approximation is represented by $K_{Ic} \sim \sigma_{Nu}\sqrt{D}$ [*Bažant and Planas*, 1998, p. 109] which suggests that an expression for σ_{Nu} be developed along with its size dependence. The equivalent crack concept is used in Appendix A to develop approximate expressions for the toughness. For alpine snow and avalanche release the true problem will be nonlinear so the partly linear expressions used in this paper must be applied with caution. In particular, it may be noted that only the ratio of toughness (K_{Ic}/K_{IIc}) is sought for practical use from this paper, and the mode II expression is $K_{IIc} \sim \tau_{Nu}\sqrt{D}$. Thus we expect that the ratio has the form (K_{Ic}/K_{IIc}) $\sim$ (σ_{N_u}/τ_{Nu}). Here the ratio is predominately determined by the nominal strength ratio from the simple one-dimensional size effect laws for mode II [*Bažant et al.*, 2003b] and another for mode I [*Bažant and Planas*, 1998] which is developed below. The nominal strength values are determined from extensive field measurements of σ_{Nu} by *Jamieson and Johnston* [1990] and estimates of τ_{Nu} from avalanche fracture lines measured in the field. We show in section 11 that the mean nominal strength ratio, σ_{Nu}/τ_{Nu}, and the mean fracture toughness ratio (K_{Ic}/K_{IIc}) derived from equivalent crack concepts are nearly the same which lends further support to our analysis. The strength estimates are the parameters with the least uncertainty in our analysis. If the toughness ratio depends mostly on the strength ratio, then the approximations used in the equivalent crack formulations may not have a major effect on the ratio.

[18] Fracture toughness is a fundamental parameter in the size effect law when avalanche failures take place. To estimate the parameters in a size effect law, it is necessary to consider the limits $D \to 0$; $D \to \infty$ representing the small size (plastic) and large size (LEFM) cases, respectively.

[19] *Bažant and Planas* [1998] and *Bažant* [2004] present a number of methods to estimate the parameters in the size effect laws. Since fracture toughness is a material property, it should not depend on whether values are obtained from a type 1 or type 2 size effect law. In this paper, tensile fracture toughness values for slab avalanches are determined from a type 2 size effect law based on laboratory data obtained from notched cantilever beam tests [*Schweizer et al.*, 2004]. The approach is by considering an equivalent crack concept from LEFM. In Appendix A, the toughness values are estimated for a type 1 size effect law used to estimate slab tensile fracture toughness using an equivalent crack concept. Combination of these results suggests that the boundary layer for crack initiation at the bottom of the slab is on the order of 20 cm.

5. Bažant's Classical Type 2 Size Effect Law for Tensile Failure Using Simple Assumptions

[20] A type 2 size effect law is introduced here in order to derive tensile fracture toughness values from notched cantilever beam tests presented by *Schweizer et al.* [2004]. Instead of a cantilever beam, consider first a notched, homogeneous dry snow sample of thickness, D, acted on by a uniaxial tensile stress, σ_N applied to a sample (Figure 2). The problem is idealized as one-dimensional, and the slab is assumed to be in rapid, elastic deformation. The snow sample is assumed to fracture as a quasi-brittle material with a fracture process zone at the tip of the crack which is of finite size. The size of the fracture process zone is related to a material constant, c_f, such that it cannot be ignored relative to the characteristic thickness, D, of the slab. The crack is taken to have total equivalent length $a_0 + c_f$ where a_0 is the continuous crack length and the length of the FPZ FPZ $\approx 2c_f$.

[21] Consider tensile extension of the crack by distance, Δa in a homogeneous slab of snow. The total energy release (per unit width) is $2k(a_0 + c_f)\Delta a(\sigma_N^2)/2E$ where k is a material constant and E is Young's modulus. To reach a propagation condition, the total energy release is balanced by the energy for crack extension (per unit width): $G_I\Delta a$ where G_I is the energy to form a unit area of tensile fracture surface (N/m). Equating these two expressions gives the simplest (type 2) one-dimensional size effect law of Bažant [*Bažant and Planas*, 1998]:

$$k(a_0 + c_f)(\sigma_N^2) = EG_I \tag{4}$$

At the instant of crack propagation, it is assumed that σ_N becomes equal to the nominal tensile strength, σ_{Nu}. The Bažant one-dimensional size effect law is then [*Bažant and Planas*, 1998]

$$\sigma_{Nu} = \frac{Bf_t'}{\sqrt{1 + D/D_0}} \tag{5}$$

where f_t' is the tensile strength of the sample, B, is a dimensionless constant and D_0 is a transitional size

(constant) between large size (brittle) and small size (nonbrittle) behavior. Both B and D_0 are assumed to depend on the fracture properties of the slab material and failure geometry but not on the characteristic size, D [*Bažant and Planas*, 1998] for geometrically similar samples ($D/a_0 = const$). Equation (5) contains two constants obtained from small and large size limits on D, respectively:

$$Bf_t' = \frac{\sqrt{EG_I}}{\sqrt{kc_f}} = const \quad \text{and} \quad D_0 = c_f \frac{D}{a_0} = const \tag{6}$$

McClung [2005a] considered an "order of magnitude" value for D_0 for alpine snow from extrapolation of results from concrete, another quasi-brittle material. For tensile specimens of concrete [*Bažant and Planas*, 1998, p. 111], $D_0 \approx 20d_a$ where d_a is maximum aggregate size. However, for alpine snow in avalanche applications, the volume fraction filled by solids is only about 20% instead of close to 85% as expected for concrete. Therefore it is suggested that an approximate size for D_0 may be $D_0 \approx 100d$ where d is maximum grain size (about 1–2 mm) or D_0 of order 10–20 cm. This order of magnitude estimate is suggested by three-point-bend experiments investigating size effects on nominal strength [*Sigrist et al.*, 2005] which imply values in the range 20–30 cm. In the expressions below for fracture toughness, D_0 is used as a parameter varying from 10–30 cm.

[22] Some important limits result from equations (1)–(3) and (5). $D \ll D_0$, then

$$\sigma_{Nu}(D \ll D_0) = Bf_t' = b_0 \tag{7}$$

where Bf_t' is the nominal tensile strength in the small size limit.

[23] *Kirchner et al.* [2004] performed experiments on small snow test samples, and they concluded that statistical size effects are very small or negligible for samples smaller than 10 cm characteristic size. Their experimental technique did not fulfill similitude requirements which limits conclusions. However, their results may provide partial support for the position here that the size effect is negligible for very small sizes. For the order of magnitude estimate of $D_0 \approx 10$ cm suggested above, this small size limit is not of practical interest for slab avalanche problems since D is normally greater than 10 cm. It is, however, of interest for interpretation of lab experiments done with small samples.

[24] If $D \gg D_0$, then from equation (5),

$$\sigma_{Nu}(D \gg D_0) = Bf_t'(D_0/D)^{1/2} \tag{8}$$

and the nominal strength converges asymptotically in the large size limit to provide estimates for linear elastic fracture mechanics (LEFM) as $\sigma_{Nu} \propto 1/\sqrt{D}$.

[25] Typical slab thicknesses of interest range for D are in the range 0.1 to several meters [e.g., *McClung and Schaerer*, 1993] so size effects become very important in avalanche problems. In order that the nominal strength in an experiment is within 5% of the asymptotic limit appropriate for LEFM (equation (8)), from equation (5) it is easily shown that $D = 10D_0$ or about 1 m if $D_0 = 0.1$ m. Such a sample size is virtually impossible to obtain in alpine snow since homogenous samples of such size do not exist: A sample layer of such thickness will consist of layers of different density, temperature, and grain structure. Size effects on tensile strength have a long history in snow mechanics starting with *Sommerfeld* [1974, 1980]. However, virtually all previous studies have been focussed on statistical size effects such as application of *Weibull* [1939, 1951] statistics to data from small homogeneous samples. A discussion of statistical size effects is beyond the scope of the present paper. *Bažant and Planas* [1998] provide an extensive discussion and analysis of statistical size effects for quasi-brittle materials.

[26] The first part of equation (6) may be expressed in terms of mode I fracture toughness:

$$K_{Ic} = \sqrt{kc_f} Bf_t' \tag{9}$$

6. Tensile Strength of Alpine Snow

[27] The formulations above are done assuming a homogeneous sample or slab of snow. In this paper, we attempt to study tensile fracture properties relevant to dry slab avalanche release from field measurements of fallen slabs and in situ estimates of tensile strength. Thus we must generalize the argument above to account for the variations in strength and toughness found in nature. The tensile strength of alpine snow depends on density, temperature, snow structure (including grain size), and rate effects. For the dry snow slab, tensile fracture takes place rapidly in a brittle manner so that variations in rate effects are expected to be minimal: All the tensile fractures happen rapidly. It is known that the Young's modulus and tensile fracture strength of the matrix material ice are weakly dependent on temperature over a wide temperature range [*Petrenko and Whitworth*, 1999]. Furthermore, for the dry slab avalanche in nature the temperature range of interest is narrow, roughly between $-20°C$ and $0°C$, so that any temperature effects are expected to be small. *Jamieson and Johnston* [1990] measured snow temperatures for the in situ tensile experiments used in the present paper, and they found that snow temperature was not statistically significant, as expected for brittle fracture [*Bažant et al.*, 2003b].

[28] *Jamieson and Johnston* [1990] measured tensile strength of alpine snow in situ, and they were able to group snow structure and grain type into two groups. The two groups consisted of (1) faceted grains and (2) those consisting of newly fallen snow, partly settled grains, rounded grains, and multilayer specimens of the three categories in group 2. For both groups they were able to get consistent (but different) relationships between tensile fracture strength and snow density for large samples stressed at rapid rates. Field experience and measurements with dry slab avalanches [e.g., *Schweizer and Jamieson*, 2001] show that the slab material (where tensile fracture initiates) almost always consists of grains within group 2. The weak layer where shear fracture initiates is often in group 1. In this paper, emphasis is on tensile failure within the slab, so estimates of tensile fracture strength are taken as a function of density for grains in group 2, from the rapid, in situ test results of *Jamieson and Johnston* [1990]. It is assumed that

rate and temperature effects are small but comparable to those in nature for rapid tensile (mode I) fracture through the slab preceded by rapid, up-slope mode II fracture within the weak layer [*McClung*, 1979, 1981].

[29] From the experiments of *Jamieson and Johnston* [1990] for rapid, unnotched, in situ tests and grain types within group 2, it is assumed that the nominal tensile strength (for the average sample size of the experiments, $(D = \overline{D})$), f_t' (in kPa), is given by

$$f_t' \approx 80(\rho/\rho_{ice})^{2.4} \tag{10}$$

where ρ is mean snow density for the layer tested and ρ_{ice} is the density of ice (917 kg/m^3). Representing tensile strength as in equation (10) is a very important assumption because it is used to develop the simple expressions for fracture toughness and characteristic size of the FPZ below and in Appendix A. Equation (10) was determined by least squares fit with 96% variance explained from the data of *Jamieson and Johnston* [1990] for snow densities between about 100–350 kg/m^3: the approximate range of interest for most slab avalanches.

[30] The experiments of *Jamieson and Johnston* [1990] may be characterized in terms of nominal tensile strength, σ_{Nu}, defined as the value of nominal stress, σ_N, at failure where

$$\sigma_N = \frac{P}{bD} \tag{11}$$

In (11), P is total downslope load applied, b, is sample width (0.45 m for the experiments), and D is sample thickness (analogous to slab thickness in the avalanche case). The applied load P included pull force applied to the sample plus downslope weight of the snow block minus bottom friction since the snow blocks were pulled on a smooth metal plate. The blocks of snow were shaped to reduce the cross sectional area but no sharp notches were cut in the samples. Therefore we assume the results represent unnotched samples.

[31] For alpine snow, P is of the form $P = P(\rho, T, rate, grain - structure)$. However, for the data of *Jamieson and Johnston* [1990], variations due to the effects of T (temperature) and rate are expected to be small so that only the density appears here since the grain structure is taken for group 2 above. Therefore $P = P(\rho)$ is taken to approximate the data. No list of values for block (layer) thickness D is given but they were always greater than 10 cm ranging up to about 30 cm. [*Jamieson*, 1989]. For constant, D, from equation (11) strict one-dimensional similitude would be implied by (8). However, since D varied with layer thickness, the experiments are slightly affected by size effects. Here, an average characteristic size of $\overline{D}$ = 20 cm (an approximate middle value) is taken to represent the experiments. Equation (7) suggests that the small sample limit for $D \ll D_0$ and a type 2 size effect law is given by

$$\sigma_{Nu}(D \ll D_0) = B\left[80\left(\frac{\rho}{\rho_{ice}}\right)^{2.4}\right] \tag{12}$$

The fracture toughness is then estimated from (9) as

$$K_{Ic} = B\sqrt{kc_f}\left[80\left(\frac{\rho}{\rho_{ice}}\right)^{2.4}\right] \text{kPa(m)}^{1/2} \tag{13}$$

In equation (13) and all subsequent formulations in this paper the units of fracture toughness are taken as kPa(m)$^{1/2}$. Equation (13) suggests that if $B\sqrt{kc_f}$ (units m$^{1/2}$) is taken to be approximately constant [*Bažant and Planas*, 1998] over the density range of the data, the fracture toughness is scale invariant with respect to multiplicative changes in ρ with power exponent 2.4. Thus a log-log plot of K_{Ic} versus ρ should be linear. However, this scale invariance is expected to break down at low and high densities outside the experimental density range of *Jamieson and Johnston* [1990]. Also, physically it may be expected that over the range of densities expected for slab avalanches (50 to 500 kg/m^3), the size of the FPZ $\approx 2c_f$ may vary with density to cause departure from scale invariance. Thus though equation (13) might be applied for rough values in simple applications, any realistic formulation on the basis of fracture mechanical measurements and principles should show deviation from the power law (or scale invariant) form. In any case, equation (10) predicts that the tensile strength of ice is 80 kPa whereas the known value is suggested of order 1000 kPa [*Petrenko and Whitworth*, 1999] for the temperature range of the experiments of *Jamieson and Johnston* [1990]. Thus any scale invariance implied by (13) will break down at high density. This is depicted schematically in Figure 3.

[32] Manufactured materials called foams display scale invariance of mechanical properties with respect to density over a wide range of densities with power law relationships such as (10) and (13) [*Gibson and Ashby*, 1999]. However, natural materials like alpine snow only display scale invariance over a fairly narrow range such as suggested here [*McClung*, 2005a]. The structure of alpine snow is not closely related to a foam through the range of densities important for avalanche applications to the transition to solid ice. Alpine snow is a bonded, granular material with a discontinuous structure not a foam as *Kirchner et al.* [2000] suggested.

[33] Support for the approximate scale invariant form (13) comes from the small size experiments on cantilever beams of alpine snow by *Schweizer et al.* [2004]. They calculated an apparent fracture toughness K_{INu}, i.e., assuming LEFM and neglecting the large size of the fracture process zone, to get an empirical expression:

$$K_{INu} = 16\left(\frac{\rho}{\rho_{ice}}\right)^{2.0} \tag{14}$$

In equation (14), calculated by least squares, percent variance explained is 96% (R^2 = 0.96) for 65 samples. Equations (13) and (14) are derived from different assumptions about geometry and mechanics including size effects but none of these assumptions should affect the scale invariance implied for density which derives from density dependence of in situ nominal strength similar to equation (10). Both (13) and (14) are derived from experiments with similar grain types, rapid rates and small temperature effects. Figure 4 shows calculations from the data from the

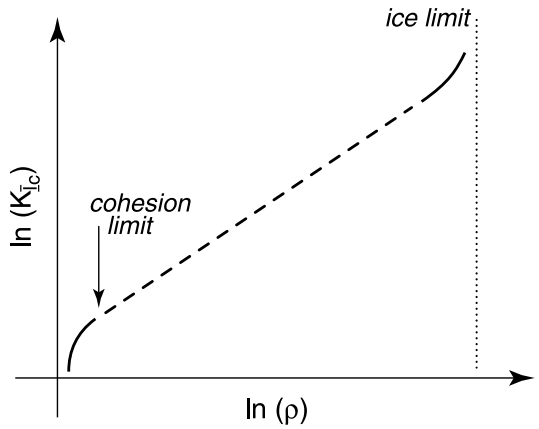

Figure 3. Schematic of log-log plot of K_{Ic} versus snow density ρ. Any scale invariance will break down at low density where cohesion approaches 0 and at high density as the limit of solid ice is approached.

cantilever experiments on a log-log plot to illustrate approximate scale invariance.

7. Evaluation of $B\sqrt{kc_f}$

[34] In order to estimate fracture toughness from equation (12), an approximate value for $B\sqrt{kc_f}$ is needed. Careful experiments are needed to validate a size effect law such as (5). Such experimental data are presently unavailable so that here approximate evaluation is done.

[35] Consider relating equations, (13) (evaluated from in situ experiments) and (14) (evaluated from lab experiments with cantilever beams). For the cantilever beams, the stress intensity factor is taken to have the approximate form $K_I = c_0\sigma_n\sqrt{\pi a}$ for a given experiment where a is crack length [*Kirchner et al.*, 2002a, 2002b; *Schweizer et al.*, 2004] and where c_0 depends on beam weight, notch length and specimen dimensions. In Appendix B, on the basis of an analysis by *Bažant and Planas* [1998, p. 110] it is shown that the apparent fracture toughness may be related to the true fracture toughness by a simple series expansion. In Appendix B, an approximate expression relating apparent and true fracture toughness is derived as equation (B6):

$$K_{Ic} = K_{INu}\left(1 + \frac{c_f}{2D_c}\right) \tag{15}$$

For a small surface crack with tensile loading perpendicular to the crack, D_c is a characteristic size given by [*Bažant and Planas*, 1998]:

$$\frac{1}{D_c} = \left[\frac{\partial \ln\left(K_I^2(\alpha)\right)}{\partial a}\right]_{a=a_0} = \frac{1}{a_0} \tag{16}$$

where $\alpha = a/D$ and $a = a_0 + c_f$.

[36] From the second part of equation (6), an approximate expression relating apparent and true fracture toughness is

$$K_{Ic} = K_{INu}\left(1 + \frac{D_0}{2D}\right) \tag{17}$$

For the experiments, assuming $D_0 = 0.1$ m and $D = 0.2$ m [*Schweizer et al.*, 2004] an "approximate" expression for fracture toughness for the lab experiments results from (14):

$$K_{Ic} = 20\left(\frac{\rho}{\rho_{ice}}\right)^{2.0} D_0 = 10 \text{ cm} \tag{18}$$

An expression for $B\sqrt{kc_f}$ by equating (13) and (18) is

$$B\sqrt{kc_f} = \frac{1}{4}\left(\frac{\rho_{ice}}{\rho}\right)^{0.4} \tag{19}$$

For three different densities the following results are obtained: $\rho = 100$ kg/m^3, $B\sqrt{kc_f} = 0.61$; $\rho = 200$ kg/m^3, $B\sqrt{kc_f} = 0.46$; and $\rho = 400$ kg/m^3, $B\sqrt{kc_f} = 0.35$. Note that there is consistency with physical expectations. As density decreases, the estimate of c_f increases slightly because of a smaller volume fraction filled by solids. Given the results of these two methods, it is suggested that $B\sqrt{kc_f} \approx 0.4$–0.6. It is assumed below that $B\sqrt{kc_f} = 0.5$ as an approximate value. The expression for fracture toughness for application to avalanche data using in situ tensile strength data is then estimated from (14) as

$$K_{Ic} = 40\left(\frac{\rho}{\rho_{ice}}\right)^{2.4} D_0 = 10 \text{ cm} \tag{20}$$

Since D_0 is unknown, we repeated the calculations for $D_0 = 30$ cm. Our results gave estimates for $B\sqrt{kc_f}$ between 0.85 ($\rho = 100$ kg/m^3) and 0.49 ($\rho = 400$ kg/m^3). Taking a middle value of about 0.67 gave another approximate estimate of toughness for application to avalanches is

$$K_{Ic} = 54\left(\frac{\rho}{\rho_{ice}}\right)^{2.4} D_0 = 30 \text{ cm} \tag{21}$$

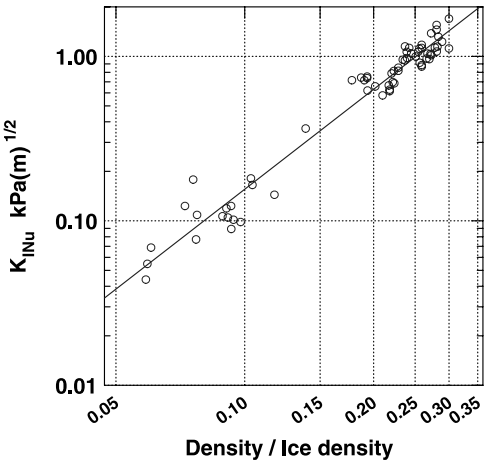

Figure 4. Values of apparent fracture toughness from lab samples, K_{INu} (kPa), versus ρ/ρ_{ice} where $\rho_{ice} = 917$ kg/m^3. The ordinate and abscissa are both logarithmic.

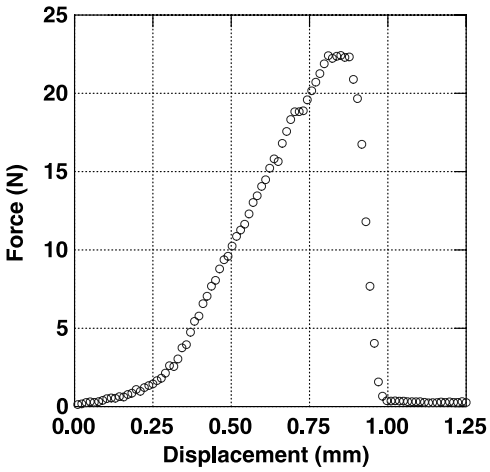

Figure 5. Force (N)-displacement (mm) curve from a three-point-bend displacement-controlled tensile fracture test on alpine snow by C. Sigrist, personal communication.

Given the range above in (20) and (21), we suggest that approximate expression applicable to avalanches is

$$K_{Ic} \approx 50\left(\frac{\rho}{\rho_{ice}}\right)^{2.4} \tag{22}$$

Equation (22) contains the prediction that the fracture toughness of ice is 50 kPa(m)$^{1/2}$ whereas *Nixon and Schulson* [1987] showed that it is about 80 kPa(m)$^{1/2}$ at −10°C, and *Dempsey et al.* [1999] suggest it is in the range 80–300 kPa(m)$^{1/2}$ This result again suggests that scale invariance will break down before the ice limit is reached (Figure 3). Equation (22) should probably not be applied beyond densities of 500 kg/m^3. Approximate verification of the power law dependence on density is given in Appendix C from independently measured Young's modulus as a function of ρ.

[37] *Bažant and Planas* [1998] provide an estimate of characteristic size of the fracture process zone, for quasi-brittle materials $R_c = \eta l_{ch}$ where η is a constant. From (13), the characteristic length [*Bažant and Planas*, 1998] is given by $l_{ch} = (K_{Ic}/f_t)^2 = B^2(kc_f)$. The values in (20) and (21), give $l_{ch} \approx 0.25$–0.5 m. These estimates are similar to values listed by *Bažant and Planas* [1998] for concrete in tension: $l_{ch} \approx 0.15$–0.40 m. Such characteristic sizes suggest that it is not possible to describe the behavior of small laboratory specimens using LEFM. This same suggestion in regard to small samples was made by *Bažant et al.* [2003b] in relation to size effects in shear for the snow slab.

[38] The softening curve is not yet known, in general, for alpine snow in tension to evaluate η for the avalanche case. However, enough data are available to enable the approximate values sought in this paper. Figure 5 shows a strain-softening curve from a three-point-bend displacement-controlled tensile fracture test performed by Christian Sigrist of the Swiss Federal Institute of Snow and Avalanche Research. The experiment shows rapid strength loss over about 0.15 mm and a linear drop from peak to zero stress. For a linear softening curve, the estimates of $R_c = (2/\pi)l_{ch}$ [*Bažant and Planas*, 1998] are in the range 15–30 cm.

[39] For the avalanche case, the characteristic scale that matters is the FPZ or length of the boundary layer thickness at the bottom of the slab. In Appendix A, it is shown that the estimates above (15–30 cm), (derived for a type 2 size effect law for notched samples), are comparable to the size of the FPZ $\approx 2c_f$: the boundary layer thickness (20 cm) estimated for a type 1 size effect law. Since $2c_f$ is a material property, it should not be dependent on whether a sample is notched or not.

8. Data From Slab Avalanche Measurements

[40] The data to estimate the parameters for fracture toughness were taken from tensile crown fracture lines from fallen snow slabs including crown (slab) thickness, D, mean slab density, $\overline{\rho}$, and slope angle ψ. Three data sets were collected: (1) 191 avalanches with a mix of three types of triggers including natural (snow loading during storms and from blowing snow), explosives, and skier triggering; (2) 48 avalanches triggered only by skiers; and (3) 60 avalanches triggered only as naturals. The applied shear stress at failure at the slab base is approximated from depth averaging as $\tau_N = \overline{\rho}\, gD\sin\psi$ where $\overline{\rho}$ is mean slab density, g is magnitude of acceleration due to gravity, and ψ is slope angle. In cases for which dynamic forces during triggering are possible (explosives and skier loading), this simple relation will be an underestimate [*McClung*, 2003]. The data are derived from *Perla* [1977], *Stethem and Perla* [1980], and the personal collections of Dr. Paul Föhn, Chris Landry, and Blyth Wright.

[41] It is important that field measurements are used from avalanches since the effective areal sample size in the weak layer is very large. This eliminates spatial variations of strength within the weak layer from the analysis. The failure strength varies within the weak layer. This was shown first by *Conway and Abrahamson* [1984] and recently by *Landry et al.* [2004], *Kronholm* [2004] and *Kronholm and Schweizer* [2003]. If weak layers involved in avalanches were homogeneous, such would imply that once loads exceed failure strength in the weak layer, avalanches would initiate everywhere. Dry slab avalanches are rare events, and either small-scale imperfections on the grain scale or homogeneous failure strength in the weak layer would produce many more avalanches than are observed. Therefore it is more likely that dry slab avalanches are generated from imperfections of macroscopic size which may be a significant fraction of the slab thickness, D [*Bažant et al.*, 2003b]. Since the data used here are from avalanches, the effective sample size in relation to the spatial scale of the weak layer is very large, and it should include within it any macroscopic imperfection which was involved in avalanche initiation. It has been known for a long time [e.g., *Perla*, 1977; *Sommerfeld*, 1980; *Jamieson*, 1995] that the shear strength within weak layers, as estimated with shear frame tests, decreases as the spatial size of the sample increases.

9. Mode II: Shear Fracture Toughness, K_{IIc}, for the Snow Slab and the Ratio K_{Ic}/K_{IIc}

[42] The aim of the present paper is to derive the ratio, K_{Ic}/K_{IIc}, of tensile fracture toughness for the slab (mode I: equation (22)) to the mode II shear fracture toughness for

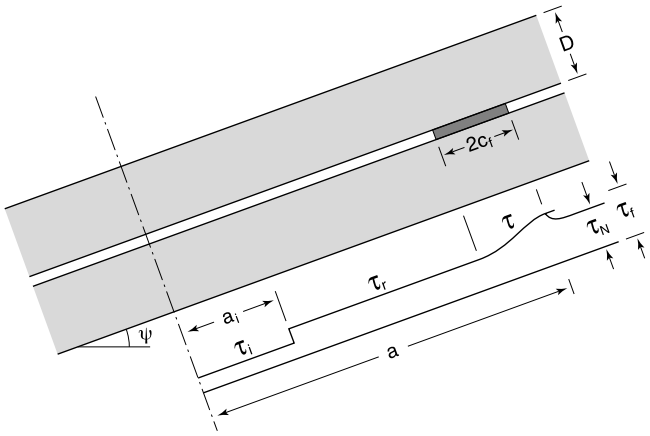

Figure 6. Schematic for mode II fracture initiation within a weak layer under a slab. Nominal shear stress, τ_N, failure stress, τ_f, residual stress, τ_r and imperfection shear stress, τ_i are shown with half lengths, a, a_i of the crack and imperfection, respectively. The fracture process zone is $2c_f$.

the slab-weak layer system. The procedure is to estimate the ratio entirely from field measured properties at the fracture lines of fallen snow slabs. Physically, it is expected that the ratio should be greater than 1 since K_{Ic} applies to a thick, strong, cohesive slab, and K_{IIc} applies to the thin weak layer from which the first propagating fracture initiates. The shear fracture toughness for dry slab avalanches has been studied by *Bažant et al.* [2003b] and *McClung* [2005a].

[43] Figure 6 shows a schematic appropriate for the cohesive crack model with an imperfection adapted from *Bažant et al.* [2003b] and *McClung* [2005a]. In Figure 6, τ_N, τ_r, τ_i are nominal, residual, and imperfection shear stresses, and a, a_0, a_i are half lengths of the crack, distance beyond the softened zone and initial imperfection length, respectively. A key dimensionless parameter is $\alpha_0 = a_0/D$ which is larger than 1 but of order 1 [*Bažant et al.*, 2003b]. The assumption is that strain softening initiates in an imperfection (or stress concentration) in the weak layer and grows under load application to reach a critical length and then propagates dynamically. After dynamic propagation up-slope, bed (weak layer) friction is removed, tensile stresses are produced in the slab with orientation of maximum principal stress parallel to the weak layer (or bed), and rapid, brittle tensile fracture occurs through the body of the slab. This process was detailed by *McClung* [1981].

[44] For the situation in Figure 6, at the instant propagation conditions are met, the stress intensity factor is replaced by the mode II fracture toughness ($K_{II} \rightarrow K_{IIc}$) and the stresses are replaced by strengths ($\tau_N \rightarrow \tau_{Nu}$) where τ_{Nu} is nominal shear strength for the weak layer or interface. An expression for the loading in Figure 6 is [*Bažant et al.*, 2003b; *McClung*, 2005a]:

$$K_{II} = \sqrt{\frac{D_0}{2}}\sqrt{1+\frac{D}{D_0}}\tau_N\left[(\alpha_0)\left\{1-\frac{\tau_r}{\tau_N}\left[1-\frac{a_i}{a}\left(1-\frac{\tau_i}{\tau_r}\right)\right]\right\}\right] \tag{23}$$

The terms within the square brackets $[(\alpha_0)\{1 - \frac{\tau_r}{\tau_N}[1 - \frac{a_i}{a}(1 - \frac{\tau_i}{\tau_r})]\}]$ yield a product of order 1 [*McClung*, 2005a], so that a simplified expression for the mode II shear fracture toughness results [*Bažant et al.*, 2003b] when $D \gg D_0$:

$$K_{IIc} = \sqrt{\frac{D}{2}}\tau_{Nu}(D) \qquad D \gg D_0 \tag{24}$$

If equation (24) is used to estimate fracture toughness for small sizes, it becomes an apparent fracture toughness: $K_{IINu} = \sqrt{\frac{D}{2}}\tau_{Nu}(D)$. From Appendix B and *McClung* [2005a], an expression relating true and apparent fracture toughness for the one-dimensional size effect law is

$$K_{IIc} = K_{IINu}\left(1+\frac{D_0}{4D}\right) = \sqrt{\frac{D}{2}}\left(1+\frac{D_0}{4D}\right)\tau_{Nu}(D) \tag{25}$$

In (25), $\tau_N = \overline{\rho}g\sin(\psi)D$ is represented by $\tau_{Nu} \rightarrow \tau_N$. It is shown by *Bažant et al.* [2003b] and *McClung* [2005a] that τ_N is a power law function (or scale invariant) of D due to very small density dependence on D and a narrow slope angle range for samples from hundreds of snow slabs.

[45] For the large size limit $D/D_0 \gg 1$, the form of (25) matches the expression given by *Bažant et al.* [2003b] and formulations of *Palmer and Rice* [1973] and *McClung* [1981] for $\alpha \rightarrow 1$. Note that the mode II slab fracture toughness depends on D: the slab thickness from the size effect law developed by *Bažant et al.* [2003b].

[46] In this paper, the values of τ_{Nu} are evaluated from full-scale slab avalanche data. Thus we do not expect a spatial size effect on τ_{Nu} from within the weak layer: The effective size (or area) within the thin weak layer is essentially infinite. However, when applied to snow slab data, the weak layer is sheared under a slab of thickness D with a finite size of the FPZ which is a significant fraction of D so a size effect results for the problem of snow slab release. The initiation is described by the type 2, mode II energetic size effect law of *Bažant et al.* [2003b]. The assumption is that the material beneath the weak layer is much stiffer than the slab above which is an approximation. The simple mode II size effect law should not be applicable to very thick slabs [*Bažant et al.*, 2003b] since it is developed for a homogeneous slab. The layered structure of deep slabs, greater than 1 meter, would require more sophisticated modelling which is beyond the scope of this paper. For the simple size effect law, given a value of D, the modelled mode II fracture toughness is a material constant.

[47] Figure 7 is a log-log plot of K_{IIc} calculated from equation (25) versus D for 191 snow slabs with a mix of triggers. Percent variance explained is 92% ($R^2 = 0.92$) for the least squares fit through the data with power exponent (or fractal dimension) 1.75 ± 0.05. An analysis of the nominal shear strength showed it is scale invariant with respect to D with power exponent 1.22. The plot suggests that K_{IIc} is approximately scale invariant with respect to multiplicative changes in D. However, such a conclusion depends on model assumptions [*McClung*, 2005a].

[48] From equation (25), a characteristic length results relative to the fracture process zone as $l_{ch} \approx (K_{IIc}/\tau_{Nu})^2 \simeq (D/2)[1 + (D_0/4D)]^2$. For values of D (D_0 = 30 cm) in the range 0.1 m $\leq D \leq$ 1 m, the estimates are $l_{ch} \approx$ 0.15–0.5 m for comparison with those in tension (0.25–0.5 m) estimated above.

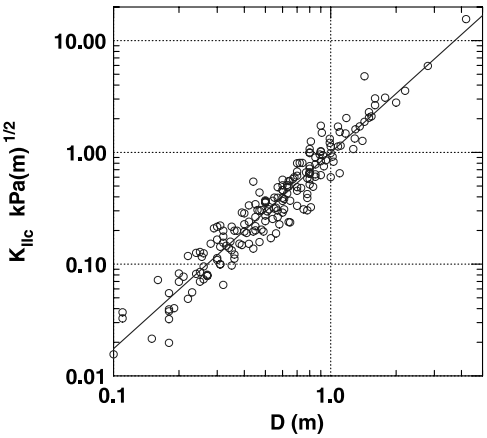

Figure 7. Model values of K_{IIc} (kPa) versus D(m) calculated from slab avalanche data. The data are from 191 slab avalanches with a mix of triggers including natural, skier, and explosive. A least squares line is shown.

[49] *McClung and Schweizer* [1999] evaluated the end zone (fracture process) size for slow strain-softening direct simple shear tests by calculating the area under the failing portion of the softening curve by the method of *Palmer and Rice* [1973]. These estimates gave values between 1.5–3 m. Later [e.g., *Bažant et al.*, 2003a] it was suggested that typically estimates based on the total area under the curve (used to estimate the fracture energy) are high by a factor of approximately 2.5. *Bažant* [2002, 2004] and *Bažant et al.* [2003a] explain that the ''initial'' fracture energy is what matters for a quasi-brittle material, and experimentally, it is normally about 40% of the total area under the complete stress-displacement curve. With this correction, the new estimates for the size of the size of the fracture process zone in shear are approximately $R_c = \eta l_{ch} \approx 0.5–1$ m. These values are consistent with the estimates of l_{ch} above from the mode II avalanche size effect law, since the constant η can be greater than or equal to 2 for quasi-brittle materials. *Bažant and Planas* [1998] suggest that η is in the range 2–5 for concrete in tension.

10. The ratio K_{Ic}/K_{IIc}

[50] The ratio of slab tensile to weak layer shear fracture toughness is expected to have important application in controlling the volume of slabs and the likelihood of slab initiation. We expect that higher ratios will imply larger slab volume and lower ratios will reduce likelihood of initiation since the slab-weak layer system becomes more homogeneous. In this section, we estimate the ratio from hundreds of slabs, and in the next section we provide limits on the applicability of the ratio in terms of slab size, D.

[51] From (22) and (25), the model ratio is approximated as

$$\frac{K_{Ic}}{K_{IIc}} = \frac{\left[50\left(\frac{\bar{\rho}}{\rho_{ice}}\right)^{2.4}\right]}{\tau_{Nu}(D)\sqrt{\frac{D}{2}}\left(1+\frac{D_0}{4D}\right)} \tag{26}$$

and where D_0 is taken as 30 cm (the approximate value for used in equation (22)). In (26), the approximation $\rho = \bar{\rho}$ is made in the numerator based on available data. The consequences of this approximation are discussed below.

[52] Table 1 contains estimated values of slab avalanche fracture toughness. In Table 1, K_{Ic} represents tensile fracture toughness in the slab, calculated from the mean value of slab density, and K_{IIc} is shear fracture toughness calculated to represent the weak layer fracture. The values in Table 1 suggest that K_{IIc} varies by almost 3 orders of magnitude and that K_{Ic} varies by more than 2 orders of magnitude for slab avalanches.

[53] Table 2 contains the descriptive statistics for the ratio K_{Ic}/K_{IIc} calculated from the slab avalanche data. The means include 95% confidence limits.

[54] For comparison, in Table 3 we provide the ratio of nominal strength σ_{Nu}/τ_{Nu} in the range for values of $D \geq 0.20$ m. In Table 3, the nominal tensile strength is given by equation (A4) of Appendix A with the cracking boundary layer (see Figure 1), D_b = 0.2 m, and nominal shear strength, τ_{Nu}, is from the full-scale avalanche data. The comparison with Table 2 is very close for the mean of the ratios. The comparison suggests that the details of the equivalent crack expansions for fracture toughness do not have a large effect on the ratio, and further support is provided for our estimates of the toughness ratio.

11. Discussion of Results: Ratio K_{Ic}/K_{IIc}

[55] The calculations of fracture toughness suggest that, on average, slab tensile toughness is about 5–7 times weak layer toughness. This kind of result is expected since the first fracture initiates in the weak layer. This result is opposite to homogeneous materials: Tensile toughness is normally less than shear toughness.

Table 1. Comparison of Slab Avalanche Fracture Toughness and Toughness From Lab Samples [*Schweizer et al.*, 2004][a]

Mode	Source	Mean kPa(m)$^{1/2}$	Range kPa(m)$^{1/2}$	Density Range kg/m^3
K_{INu}	65 lab samples	0.74 ± 0.11	0.04–1.7	50–275
K_{Ic}	60 natural trigger	2.15 ± 0.56	0.24–13	100–515
K_{IIc}	60 natural trigger	0.62 ± 0.20	0.06–4.8	100–515
K_{Ic}	191 mix of triggers	1.67 ± 0.20	0.07–9.5	60– 460
K_{IIc}	191 mix of triggers	0.71 ± 0.20	0.02–17	60–460
K_{Ic}	48 skier trigger	1.59 ± 0.28	0.19–3.9	90–315
K_{IIc}	48 skier trigger	0.46 ± 0.17	0.3–3.2	90–315

[a]The mean values include 95% confidence limits.

Table 2. Ratio K_{Ic}/K_{IIc} Calculated From Dry Slab Avalanche Data

Mean Ratio K_{Ic}/K_{IIc}	Range K_{Ic}/K_{IIc}	Source
6.0 ± 2.3	0.5–65	60 natural trigger
5.2 ± 0.9	0.3–45	191 mix of triggers
6.6 ± 2.2	1–43	48 skier trigger

[56] Figures 8 shows the ratio K_{Ic}/K_{IIc} for the slab data from a mix of triggers. Similar plots were constructed for the other data sets. These plots show that for most (more than 95%) of the slabs the ratio exceeds 1. However, the plots also show that there is a consistent relation between the ratio and the slab depth D: The ratio drops as D increases. This is a consequence of the simple size effect laws used to calculate the toughness. For large slabs with D greater than 1 m the ratio can be less than 1 which is not expected physically. The one-dimensional size effect law for mode II developed by *Bažant et al.* [2003b] strictly applies only as long as the slab dimension, D, is not too thick. In the field, very large sizes imply a layered (nonhomogeneous) structure to the slab which would require more complex modelling than is contained in the simple shear fracture size effect law of *Bažant et al.* [2003b].

[57] If the toughness ratios in Table 2 are calculated for slabs with $D \leq 1$ m, then virtually all of the ratios are greater than or equal to 1. The least squares line in Figure 8 yields the prediction that the ratio lies between 34 (0.1 m slab),12 (0.2 m slab) and 1.7 (1 m slab). Table 3 contains similar calculations for all three data sets. *Bažant* [2002, p. 43] shows that the simple type 1 size effect law (presented in Appendix A), is valid for $D \geq D_b \approx 2c_f$ where the cracking boundary layer thickness $D_b \approx 20$ cm (Appendix A). Also, the simple asymptotic expansion in equation (25) for K_{IIc} should not be accurate for values of D as low as 0.1 m. Thus the validity of the ratio calculations is in the approximate range 0.20 m $\leq D \leq$ 1 m considering both size effect laws.

[58] The calculations represented in Tables 2 and 4 suggest that on average, the ratio K_{Ic}/K_{IIc} may be expected to lie between 2 and 15 with mean values 5–7 for D between 0.2 m and 1 m. The calculations also suggest a higher ratio "on average" for thinner slabs with values as high as even 30–40 for thin slabs. However, slabs as thin as 0.1 m are outside the validity of the type 1 size effect law. The decrease in the ratio on average conforms with what is known from the magnitude-frequency relation for D [*McClung*, 2003] and concepts about K_{IIc} for the snow slab. The value of K_{IIc} increases rapidly with avalanche size, D, because of fracture energy gain under the load of the slab to make avalanche frequency decrease lognormally with size. The lower the ratio K_{Ic}/K_{IIc} with increasing D, the less likely, on average, is slab release. Large slabs ($D > 1$ m) are rarely encountered when the "average" conditions are not present: deeply buried weak layers which persist for long periods such as surface hoar, faceted crystals, and depth hoar which gain fracture energy slowly under load by bonding.

Table 3. Estimates of the Ratio of Nominal Tensile to Nominal Shear Strength From Field Data

Mean ratio σ_{Nu}/τ_{Nu}	Range σ_{Nu}/τ_{Nu}	Source
5.3 ± 1.0	0.7–18	57 natural trigger
5.2 ± 0.6	0.7–30	180 mix of triggers
6.4 ± 1.7	1.8–30	45 skier trigger

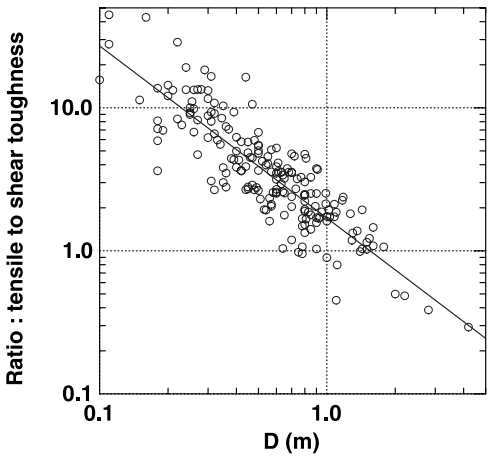

Figure 8. Model ratio of K_{Ic}/K_{IIc} versus D(m) for the same avalanches as Figure 7. A least squares line is shown.

[59] Power law relationships were calculated from the estimates on the plots by least squares fits between $\ln(K_{Ic}/K_{IIc})$ and $\ln(D)$. The least squares fits all showed the ratio had the form

$$\frac{K_{Ic}}{K_{IIc}} \propto D^{-\beta} \tag{27}$$

where β is a constant close to 1. The results are shown in Table 5. The results in Table 5 may be simply understood from the model equation (26).

$$\frac{K_{Ic}}{K_{IIc}} \propto \frac{\overline{\rho}^{2.4}}{\overline{\rho} D^{1.5}} \propto \frac{\overline{\rho}^{1.4}}{D^{1.5}} \tag{28}$$

The data show that $\overline{\rho} \propto D^{\gamma}$ where $0 < \gamma < 1/4$ depending on triggering conditions to yield an expression $K_{Ic}/K_{IIc} \sim D^{-\beta}$ where $1.15 < \beta < 1.50$. Therefore the results are due to model assumptions (the size effect laws in tension and shear) in combination with the field data. These calculations illustrate how the model predictions produce low values of the ratio as D increases. For very large slabs, e.g., $D > 1$ m, the ratio can drop below 1.

[60] Another related reason for the low ratios for thick slabs is based on the density assumptions. The values of ρ were taken as *mean* slab density in the calculations of K_{Ic}. Since tensile fracture is expected to initiate at the slab base for a type 1 size effect law, a value of the density near the slab base should be more appropriate. Since density increases with depth in alpine snow, it is expected that basal density can be higher than mean slab density for thick slabs. This would increase K_{Ic} in the ratio calculations, particularly for thick slabs. Density profiles taken at the crowns of large slab avalanches show that the density at the base can be twice the mean density [*Haefeli*, 1954] but this is an exception. *Perla* [1977] and *Stethem and Perla* [1980]

Table 4. Ratio K_{Ic}/K_{IIc} for Three Different Values of D From Least Squares Lines

D = 0.1 m	D = 0.2 m	D = 1 m	Source
38	15	1.7	60 natural trigger
34	12	1.7	191 mix of triggers
34	14	1.7	48 skier trigger

reported $\overline{\rho}$ and density near the slab base, ρ_B, for 76 dry slabs with a mix of triggers. Our analysis showed that the ratio $\rho_B/\overline{\rho}$ had a mean value of 1.21 ± 0.07, and a range of 0.5–2. There is, however, no significant correlation of the ratio with slab depth D in these data. It might be possible to develop a relation between mean slab density and density at the base as a function of D to get better estimates based on this effect, but such is beyond the scope of the present paper. On average, the 76 values from the slab data suggest slight increases in K_{Ic} over our estimates above but with wide variations, particularly for thin slabs. For the 76 slabs, least squares regression gave $\rho_B \propto D^{0.36}$; $\overline{\rho} \propto D^{0.32}$ which reduces the value of β in equation (28) from the minimum of 1.15 to about 0.96. Thus this effect gives only slight reduction in the dependence of the ratio of toughness as a function of D based on the available data.

12. Conclusions and Discussion

[61] On the basis of lab tests, in situ strength tests, and variations found in field data from snow slabs, fracture toughness in both the weak layer shear (mode II) and slab tension (mode I) are expected to vary by approximately 2–3 orders of magnitude in nature. The mode I estimates of fracture toughness are gained from empirical fits to apparent fracture toughness, K_{INu}, from cantilever beam tests of *Schweizer et al.* [2004]. *Sigrist et al.* [2005] present apparent fracture toughness from notched three-point-bending tests, and they suggest that their values are about 25% higher than from cantilever beam tests with considerable scatter shown for both data sets. This is only one source of uncertainty of several which limits the precision of our conclusions.

[62] Slab tensile toughness, K_{Ic}, is estimated to be, on average, about 5–7 times weak layer shear toughness, K_{IIc}. Wide variations are expected, with the ratio exceeding more than 10 and perhaps higher. The theoretical estimates suggest that, on average, the ratio decreases with slab thickness, D, which is qualitatively what we observe in nature. It suggests that, on average, thinner slabs are much more common than thick slabs which is observed [*McClung*, 2003]. Again, since our estimates are based mostly on field data and the simplest possible models, high precision cannot be expected. We also calculated the ratio of tensile strength and shear strength (see Table 3) taking into account the simple size effect laws, and we found that the ratio of tensile strength to shear strength, on average, is virtually identical to the toughness ratio when the uncertainty is taken into account, i.e., the average values range between 5–6. This analysis provides further support for our approximate values of toughness ratio.

[63] For both the size effect laws in this paper, equivalent LEFM has been used to yield simple formulae. Both size effect laws are identical to the original size effect laws presented by *Bažant and Planas* [1998] for quasi-brittle materials in general. The mode II law has a one-to-one relationship to the cohesive crack model [*Bažant et al.*, 2003b]. Correspondence between the cohesive crack model and the simple type 1 size effect law for mode I (equation A4) is discussed by *Bažant* [2002, pp. 195–199]. Thus we conclude that both the simple size effect laws in this paper, are compatible with the cohesive crack model in spite of the simple LEFM forms. In order to accurately evaluate the fracture parameters for the cohesive crack model, the strain-softening curve in the FPZ must be known. However, this would be nearly impossible to determine in the field. Since we seek only rough estimates from field measurements such accuracy is beyond the scope of our work. It would be very difficult to determine a strain-softening curve which is generally applicable for alpine snow for either mode I or mode II.. The cohesive crack model lumps all the inelastic deformation in the FPZ into a line of finite width and length. The advantage is that all the body volume can be treated as linear elastic, and it is known that little error is involved by lumping the failure process whenever the softening damage localizes into a narrow band [*Bažant*, 2002, p. 177]. For the snow slab, mode II fracture is either within a thin weak layer or at the boundary (line) between the weak layer and the slab so the failure will be localized into a thin band. Mode I fracture is rapid, through the body of the slab, and the connection between the cohesive crack model assumptions and the actual damage localization into a narrow band may be less obvious than for mode II. However, tensile avalanche fracture lines are straight (no meandering) and perpendicular to the weak layer [*McClung*, 1981, 2005a] at any scale D. These field observations suggest random statistical effects are not having a major role, possible concentration of deformation and stresses into a narrow band, as shown by lack of meandering, and the fracture sequence (weak layer shear first, then tensile crown fracture) is the same independent of slab thickness scale, D [*McClung*, 2005a].

[64] Our theoretical results suggest scale invariance with respect to multiplicative changes in K_{IIc} with D and for K_{Ic} with ρ but these are theoretical predictions and only approximate. However, the scale invariant relations may suffice as approximations for practical use. The size effect laws of *Bažant* [2004] contain material properties (e.g., c_f or fracture process zone size) to evaluate the constants, and surely these must vary somewhat over the density and grain size range appropriate for the snow slab (50–500 kg/m^3). Thus some dependence on a characteristic length is implied which is absent from the power law relations. Also, scale invariance for the formulations must break down for very low and very high values of the parameters D [*McClung*, 2005a] and ρ (Figure 3).

Table 5. Depth Dependence of the Ratio $K_{Ic}/K_{IIc} \propto D^{-\beta}$ Implied by the Models Used With β (With 95% Confidence Limits) Evaluated by Least Squares

Source	β	% Variance explained
60 natural trigger	1.34 ± 0.24	67
191 mix of triggers	1.20 ± 0.10	75
48 skier trigger	1.30 ± 0.22	75

[65] For slab tensile failure, the size scale that matters is the estimate of the fracture process zone (FPZ) at the bottom of the slab. Once the FPZ is formed under high tensile stress, tensile fracture through the body of the slab is imminent. We estimate that the size of the FPZ $\approx 2c_f$ is in the approximate range 15–30 cm. In slab avalanche formation, there will be stress redistribution from a finite sized FPZ before macrocrack initiation. This will happen dynamically as the shear fracture propagates within the weak layer at a significant fraction of the shear wave speed [*McClung*, 2005b]. The size estimate of the FPZ is of immense significance for field evaluation of snow slab instability since it gives an approximate length scale over which hardness characteristics and layer changes are important. For example, field observations suggest that changes in hardness between the weak layer and slab will determine initiation likelihood and also expected slab dimensions. *McCammon and Schweizer* [2002] obtained this result empirically from a statistical analysis of snow profiles near skier triggered avalanches but they had no estimate of the length scale.

[66] The size of the FPZ for weak layer failure (mode II) is another length scale of importance for avalanche forecasting since it defines limitations on applicability of in situ instability tests. The size of the FPZ for weak layer shear failure (mode II) is estimated to be on the order of 0.15–1 m from shear strain-softening experiments [*McClung and Schweizer*, 1999] applied to the cohesive crack model and the characteristic size estimates in this paper from slab avalanche data. *Bažant et al.* [2003b] estimated that the length of the shear crack at fracture initiation is on the order of the slab thickness D. Thus these three estimates are comparable within the appropriate accuracy. The small, but macroscopic, size for mode II fracture initiation is what casts avalanche forecasting into a risk-based activity by limiting the applicability of in situ instability tests. The same concept will apply to prediction of flake landslides and rock avalanches making it nearly impossible to locate or measure the properties where failure initiates.

[67] Alpine snow is especially prone to viscous deformation unless the deformation rate is very high. *Bažant et al.* [2003b] discussed the issue of viscous deformation for the shear (mode II) size effect law used in this paper. For tensile (mode I) failure, the requirement for purely elastic deformation, as assumed in this paper, is fulfilled for avalanche failures since the tensile stresses are generated dynamically as the shear crack propagates in the weak layer at s significant fraction of the shear wave speed [*McClung*, 2005b].

Appendix A: Fracture Toughness for Type 2 and Type 1 Tension Failures From LEFM-Equivalent Crack Concepts

A1. Type 2 Size Effect Law

[68] Figure 2, shows a simple notched sample with an applied tensile stress for which it is appropriate to derive a type 2 size effect law. In LEFM, a dimensionless energy release function characterizes the effect of geometry. It is defined as $g(\alpha) = k^2(\alpha)$ where $\alpha = (a_0 + c_f)/D = a/D = \alpha_0 + c_f/D$ is the relative length of the crack. The mode I stress intensity factor may be written $K_I = \sigma_N k(\alpha)\sqrt{D}$. To obtain asymptotic expressions for the fracture toughness, an equivalent LEFM crack is placed in the FPZ, and the general expression is used: $\sigma_{Nu} = K_{Ic}/[Dg(\alpha)]^{1/2}$ with expansion in a Taylor series about the ratio c_f/D [*Bažant*, 2002, 2004] where $g(\alpha) = g(\alpha_0) + g'(\alpha_0)c_f/D + \ldots$. The fracture parameters for the type 2 size effect law are then

$$D_0 = c_f g'(\alpha_0)/g(\alpha_0); K_{Ic} = Bf_t'[D_0 g(\alpha_0)]^{1/2} = Bf_t'\left[c_f g'(\alpha_0)\right]^{1/2} \tag{A1}$$

where the toughness is expressed from the limit $D \to 0$ in the type 2 size effect law and has the same form as equation (9).

A2. Type 1 Size Effect Law

[69] Figure 1 shows the physical situation expected for a type 1 failure. For a type 1 failure the crack length $a_0 = 0$, and the LEFM-equivalent crack length is equal to c_f. For such a crack, the energy release rate is zero. The value of $g(\alpha_0) = g(0) \equiv 0$, and the Taylor series expansion gives

$$g(c_f/D) = \lim_{\alpha_0 \to 0}\left[g(\alpha_0) + g'(\alpha_0)(c_f/D) + \frac{1}{2!}g''(\alpha_0)(c_f/D)^2 + \ldots\right] \tag{A2}$$

In the large size limit, $[D \to \infty;\ \sigma_{Nu} \to \sigma_{N\infty}]$, the fracture toughness is given by

$$K_{Ic} = \sigma_{N\infty}\left[c_f g'(0)\right]^{1/2} \tag{A3}$$

Note that the asymptotic expressions for the fracture toughness for type 2 in (A1) and type 1 in (A3) arise from the limits of $D \to 0$; $D \to \infty$, respectively. The values are obtained as functions of the small size limit (type 2) and large size limit (type 1) nominal strength estimates. For a crack starting a smooth surface, $g'(0) = (1.12)^2\ \pi = 3.94$ independent of shape of the "structure" analyzed if $\sigma_{N\infty}$ is taken as the mean value of tensile strength perpendicular to the crack face at the point of cracking [*Bažant and Planas*, 1998, p. 267]. Thus with empirical values of fracture toughness, $K_{Ic}(\rho)$, and a value for $\sigma_{N\infty}$, the boundary layer thickness is $D_b \approx 2c_f$d.

[70] From *Bažant* [2002, 2004], the simplest type 1 size effect law is

$$\sigma_{Nu} = \sigma_{N\infty}\left(1 + \frac{D_b}{D}\right) \approx \sigma_{N\infty}\left(1 + \frac{2c_f}{D}\right) \tag{A4}$$

where

$$\sigma_{N\infty} \approx f_t' = 80\left(\frac{\rho}{\rho_{ice}}\right)^{2.4} \tag{A5}$$

from the in situ tensile experiments of *Jamieson and Johnston* [1990].

[71] The fracture toughness for the type 1 size effect law is given by

$$K_{Ic} = 80\left(\frac{\rho}{\rho_{ice}}\right)^{2.4}\sqrt{g'(0)c_f} = 50\left(\frac{\rho}{\rho_{ice}}\right)^{2.4} \tag{A6}$$

where equation (22) has been used to estimate the toughness calibrated from the notched cantilever beam experiments of [*Schweizer et al.*, 2004]. With $\sqrt{g'(0)} = 1.985$ this gives $c_f \approx 0.1$ m or a boundary layer thickness at the bottom of the slab of about 20 cm. This size estimate (20 cm) approximately matches the (unnotched) average sample sizes of *Jamieson and Johnston* [1990]. *Bažant* [2002] suggests that the validity of the simple size effect law (A4) is in the range $D \geq D_b \approx 20$ cm.

[72] The simple size effect relation (A4) suggests that for a 50 cm slab subject to a strain gradient, nominal strength values would be 40% higher than the in situ tensile strength estimates of *Jamieson and Johnston* [1990]. For uniform tension (zero strain or stress gradient as assumed in the direct unnotched uniaxial tests), there is no highly stressed boundary layer ($D_b = 0$), and the nominal tensile strength values in (A4) coincide with the data of *Jamieson and Johnston* [1990].

[73] The analysis highlights an important concept in the use of the in situ tensile strength data of *Jamieson and Johnston* [1990]. For a type 1 size effect law, the data are taken to represent the strength in a boundary layer of about 20 cm thick, the approximate average size of their samples, at the bottom of the slab where the initial crack forms.

Appendix B: Relating True and Apparent Fracture Toughness for Mode I and Mode II

[74] When fracture toughness is calculated from a model assuming LEFM for a material which has a finite sized fracture process zone as expected for alpine snow, the result gives an apparent fracture toughness. The concept of fracture toughness (called true fracture toughness) is that it applies to brittle fracture with LEFM assumed. For the size effect laws in this paper, it is appropriate to assume that LEFM applies in the limit of large (D) size. However, simple approximate methods are available to relate apparent fracture toughness to true fracture toughness for quasi-brittle materials as shown by *Bažant and Planas* [1998] using the equivalent elastic crack concept in their book. The development here follows the logic in *Bažant and Planas* [1998, pp. 108–111], but it is slightly modified as a result of a personal communication from Z.P. *Bažant*, 2004.

[75] From *Bažant and Planas* [1998], the true fracture toughness is defined as

$$K_{Ic} = \sigma_{Nu}\sqrt{D}k(\alpha_{ec}) \tag{B1}$$

where the equivalent crack length is defined as $a_e = a_0 + \Delta a_e$ with a_0 as initial crack length and Δa_e as extension. For the critical crack length, $\alpha_{ec} = \alpha_0 + \Delta a_{ec}/D$. It is shown in *Bažant and Planas* [1998] that $\Delta a_{ec} \approx c_f \ll D$ and a two term Taylor series expansion gives

$$k(\alpha_{ec}) \approx k(\alpha_0) + k'(\alpha_0)\frac{c_f}{D} \tag{B2}$$

From *Bažant and Planas* [1998], the apparent fracture toughness is given by

$$K_{INu} = \sigma_{Nu}\sqrt{D}k(\alpha_0) \tag{B3}$$

From (B1), (B2), and (B3), an expression relating true and apparent fracture toughness results:

$$K_{Ic} = K_{INu}\left(1 + \frac{c_f}{D}\frac{k'(\alpha_0)}{k(\alpha_0)}\right) \tag{B4}$$

From *Bažant and Planas* [1998], an intrinsic, characteristic size D_c is defined as

$$\frac{1}{D_c} = \left[\frac{\partial \ln K_I^2(\alpha)}{\partial a}\right]_{a=a_0} \tag{B5}$$

and the asymptotic deviation from LEFM is expressed as

$$K_{Ic} = K_{INu}\left(1 + \frac{c_f}{2D_c}\right) \tag{B6}$$

Equations (B4) and (B6) are similar to equations in *Bažant and Planas* [1998] but they have broader applicability in terms of asymptotic behavior as $D_c \to 0$. For mode II, the same formalism will apply but, of course, the size effect law has a different form [*Bažant et al.*, 2003b]. *McClung* [2005a] has given the appropriate form. For either mode I or mode II the simple expressions used to estimate fracture toughness (equations (17) and (25)) are equivalent to truncation of a Taylor series after two terms, and thus they must be regarded as approximations, particularly for thin slabs. However, uncertainty about the transitional scaling size, D_0, is probably a larger effect than retention of more terms in the series. In the use of equations (17) and (25), we have assumed $D_0 \approx 30$ cm as near a maximum expected to account for the fact that the expressions may be underestimates since further terms in the Taylor series are positive.

Appendix C: Power Law Dependence of Young's Modulus on Density for Alpine Snow

[76] In this Appendix, the power law density dependence of Young's modulus for alpine snow is derived simply from the proposed fracture toughness relation of equation (22). Since no field measurements of K_{Ic} are available, it is important to check for consistency with other measured properties of snow for verification. The fundamental definition of fracture toughness was given by *Irwin* [1958],

$$K_{Ic} = \sqrt{E'G_I} \tag{C1}$$

where $E' = E/(1 - \nu^2)$ in plane strain and $E' = E$ in plane stress with E Young's elastic modulus and ν as the Poisson ratio. For low-density snow, *Mellor* [1975] suggests $\nu < 0.2$ so we approximate $E' \approx E$ for plane problems. In (C1), G_I is the fracture energy: the energy to form a unit area fracture surface in the material (N/m). Equation (22) represents an approximate expression for fracture toughness in tension derived from field experiments in the density range: 100–350 kg/m^3. For densities in this range we approximate the fracture energy as a constant multiple of the value for ice which is consistent with the assumptions to derive equation (22):

$$G_{I(snow)} \approx C_0 G_{I(ice)} \tag{C2}$$

where fracture energies for snow and ice are defined. From (C1), the ratio of fracture toughness of snow and ice is then

$$\frac{K_{Ic}}{K_{Ic(ice)}} = \left(\frac{C_0 E'}{E'_{ice}}\right)^{1/2} \tag{C3}$$

Now from equation (22) substituting for K_{Ic}, assuming $K_{Ic(ice)}$; E'_{ice} as constants [*Petrenko and Whitworth*, 1999] and solving for the modulus gives the density dependence for the modulus of snow:

$$E'(\rho) = C\left(\frac{\rho}{\rho_{ice}}\right)^{4.8} \tag{C4}$$

It can be shown [*Schweizer et al.*, 2004; *Mellor*, 1975; *Kojima*, 1954] that the known data on Young's modulus for snow follow this density dependence in the principal range of interest: densities between 150–350 kg/m^3. *Mellor* [1975] presents a range of Young's modulus with snow density, on the basis of the data of *Kojima* [1954]. The upper range of the data is approximately matched with $C = 40 \times 10^5$ kPa and the lower range with $C = 18 \times 10^5$ kPa. *Camponovo and Schweizer* [2001] measured the shear modulus of alpine snow in the range 215–255 kg/m^3. Assuming a Poisson ratio of about 0.2 yields a value for $E' \approx 15 \times 10^2$ kPa for an average density of 235 kg/m^3. From equation (C4) the estimated value of $C = 10 \times 10^5$ kPa. Of importance is that the relation (C4) matches the power law dependence of what is known about the Young's modulus of snow. *Mellor* [1975] suggests that Kojima's data are for well-bonded, well-settled snow. The reported data on Young's modulus show that variations up to a factor of 3.5 may be expected for the same density.

[77] The constant C_0 in (D4) may be expressed in terms of parameters for ice, and equation (22) as

$$C_0 = \left(50/K_{Ic(ice)}\right)^2 \left(E'_{ice}/C\right) = 2500/\left(CG_{I(ice)}\right) \tag{C5}$$

Dempsey et al. [1999] (p. 333) estimate the fracture energy of freshwater ice for large sizes as about 3 N/m. Taking the values for C suggested by the data reported by *Mellor* [1975] and the estimate from *Camponovo and Schweizer* [2001] gives values $C_0 \approx 0.2–0.8$ or that the fracture energy of snow is less than for large samples of freshwater ice. However, the analysis is not accurate enough to estimate a value that can be used in practice. Uncertainties about the data from all four sources, uncertainties about the ice parameters and the approximations combined in the ratio (C5) suggest that C_0 is only an order of magnitude estimate at best.

[78] The fracture energy for the stable fracture of a single crystal of freshwater ice at temperatures slightly less than 0°C is given by twice the surface energy of ice: $2\gamma_{se}$ = 0.218 N/m [*Ketcham and Hobbs*, 1969; *Dempsey and Palmer*, 1999]. Taking the empirical values of E' from (C4) and the ranges for C snow provided by the data from *Mellor* [1975], gives an empirical, hypothetical equation for fracture toughness of single crystals. Using Irwin's relation (C1) with the substitution $G_I \rightarrow 2\gamma_{se}$ [*Rice*, 1968, p. 234] gives

$$K_{Ic(sc)} = A\left(\frac{\rho}{\rho_{ice}}\right)^{2.4} \tag{C6}$$

where A is in the range 20–30 kPa(m)$^{1/2}$. Comparison with equation (22) suggests $K_{Ic}/K_{Ic(sc)} \approx 2$ and an alternate way to view it. Given the modulus for alpine snow, its mode I fracture toughness is predicted to be about twice that for fracture of single ice crystals. From data on large samples of freshwater ice [*Dempsey et al.*, 1999], a comparable calculation shows that the fracture toughness of 300 kPa(m)$^{1/2}$ is about 6 times that for single crystals [*Dempsey and Palmer*, 1999].

[79] *Bažant and Planas* [1998, p. 164] suggest that the fracture energy may be estimated approximately as 1–1.67 times the product of f'_t, and displacement over which the softening curve drops to zero. For a density of 200 kg/m^3 and displacement 0.15 mm (from Figure 5), this rule of thumb yields a fracture energy for snow of 0.3–0.5 N/m if tensile strength is estimated from equation (10). Comparison yields an order of magnitude for $C_0 \approx 0.1–0.2$ in equation (C2) using a fracture energy of 3 N/m for large samples of freshwater ice suggested by *Dempsey et al.* [1999] or about twice the fracture energy for single crystals of freshwater ice as suggested above.

Notation

a	crack length, m.
a_e	equivalent crack length, m.
a_0	continuous crack length, m.
a_i	initial imperfection length, m.
b	tensile sample width, m.
b_0, b_1, b_2	constants in energetic size effect laws.
B	dimensionless size effect fracture parameter.
c_f	half length of failure process zone, m.
d	maximum snow grain size, mm.
d_a	maximum concrete aggregate size, mm.
D	nominal size (thickness) of snow slab, m.
D_b	boundary layer thickness in type 1 size effect law, m.
D_0	transitional fracture parameter size, m.
D_c	characteristic size, m.
$\overline{D}$	mean sample thickness of tensile experiments, m.
E	Young's modulus, kPa.
E'_{ice}	effective modulus of ice in plane strain or plane stress, kPa.
E'	effective modulus in plane strain or plane stress, kPa.
f'_t	tensile strength, kPa.
g	magnitude of acceleration due to gravity (9.81 m/s^2).
$g(\alpha)$	dimensionless energy release rate in equivalent crack formulations.
G_I	mode I fracture energy, N/m.
$G_{I(ice)}$	mode I fracture energy of ice, N/m.
$G_{I(snow)}$	mode I fracture energy of snow, N/m.
k	dimensionless fracture parameter in mode I size effect law.

K_I mode I stress intensity factor, kPa(m)$^{1/2}$.
K_{Ic} mode I fracture toughness, kPa(m)$^{1/2}$.
$K_{Ic(ice)}$ mode I fracture toughness of ice, kPa(m)$^{1/2}$.
K_{INu} mode I apparent fracture toughness, kPa(m)$^{1/2}$.
K_{II} mode II stress intensity factor, kPa(m)$^{1/2}$.
K_{IIc} mode II fracture toughness, kPa(m)$^{1/2}$.
l_{ch} characteristic size of fracture process zone, m.
P tensile applied load, kN.
$P_{\max}$ tensile applied load at failure, kN.
R_c characteristic size of the fracture process zone (m).
T snow temperature, °C.
α dimensionless crack length = a/D.
α_{ec} dimensionless-equivalent crack length = a_e/D.
α_0 dimensionless continuous crack length = a_0/D.
γ_{se} surface energy of ice = 0.109 N/m.
η dimensionless constant for estimating $R_c = \eta l_{ch}$.
υ dimensionless Poisson ratio.
ρ snow density, kg/m^3.
ρ_B snow density at the bottom of a snow slab, kg/m^3.
ρ_{ice} ice density, 917 kg/m^3.
σ_N nominal tensile stress, kPa.
σ_{Nu} nominal tensile strength, kPa.
$\sigma_{N\infty}$ mean boundary layer tensile strength, kPa.
τ_N nominal shear stress, kPa.
τ_{Nu} nominal shear stress, kPa.
τ_r residual shear stress, kPa.
τ_i imperfection shear stress, kPa.
ψ slope angle (^{0}).

[80] **Acknowledgments.** This work was supported by the Natural Sciences and Engineering Research Council of Canada, Canadian Mountain Holidays, the University of British Columbia, and an Izaak Walton Killam Research Fellowship at UBC for D. McClung. Financial support was also derived from the WSL, Swiss Federal Institute for Snow and Avalanche Research, for D. McClung's visit to the Institute.

References

Bažant, Z. P. (2002), *Scaling of Structural Strength*, 280 pp., Hermes Penton Ltd., London, U.K.
Bažant, Z. P. (2004), Scaling theory for quasibrittle structural failure, *Proc. Natl. Acad. Sci. U. S. A.*, *101*(37), 13,400–13,407.
Bažant, Z. P., and J. Planas (1998), *Fracture and Size Effect in Concrete and Other Quasibrittle Materials*, 616 pp., CRC Press, Boca Raton, Fla.
Bažant, Z. P., Q. Yu, and G. Zi (2003a), Choice of standard fracture test for concrete and its statistical evaluation, *Int. J. Fract.*, *118*, 303–337.
Bažant, Z. P., G. Zi, and D. McClung (2003b), Size effect law and fracture mechanics of the triggering of dry snow slab avalanches, *J. Geophys. Res.*, *108*(B2), 2119, doi:10.1029/2002JB001884.
Camponovo, C., and J. Schweizer (2001), Rheological measurements of the visco-elastic properties of snow, *Ann. Glaciol.*, *32*, 44–50.
Conway, H., and J. Abrahamson (1984), Snow stability index, *J. Glaciol.*, *30*(106), 321–327.
Dempsey, J. P., and A. C. Palmer (1999), Non-universal scaling of arctic fractures, paper presented at the 15th International Conference on Port and Ocean Engineering Under Arctic Conditions, Helsinki University of Technology, Espoo, Finland, 23–27 August.
Dempsey, J. P., S. J. DeFranco, R. M. Adamson, and S. V. Mulmule (1999), Scale effects on the in-situ tensile strength and fracture of ice. part I: Large grained freshwater ice at Spray Lakes Reservoir, Alberta, *Int. J. Fract.*, *95*, 347–366.
Gibson, L. J., and M. F. Ashby (1999), *Cellular Solids: Structure and Properties*, 2nd ed., 510 pp., Cambridge Univ. Press, New York.
Griffith, A. A. (1921), The phenomena of rupture and flow in solids, *Philos. Trans. R. Soc., Ser. A*, *221*, 163–197.
Griffith, A. A. (1924), The theory of rupture, *Proceedings of the First International Congress for Applied Mechanics*, edited by C. B. Biezino, and J. M. Burgers, pp. 55–63, Waltman Uitgevery, Delft, Netherlands.
Haefeli, R. (1954), Snow mechanics with references to soil mechanics, in *Snow and Its Metamorphism*, chap. 2, pp. 67–219, transl. 14, Snow Ice and Permafrost Res. Estab., U.S. Army, Willamette, Ill.
Irwin, G. R. (1958), Fracture, in *Handbuch der Physik*, vol. 6, edited by W. Flügge, pp. 551–590, Springer, New York.
Jamieson, J. B. (1989), In-situ tensile strength of snow in relation to slab avalanches, M.S. thesis, 142 pp., University of Calgary, Canada.
Jamieson, J. B. (1995), Avalanche prediction for persistent snow slabs, Ph.D. thesis, 258 pp., University of Calgary, Canada.
Jamieson, J. B., and C. D. Johnston (1990), In-situ tensile strength of snowpack layers, *J. Glaciol.*, *36*(122), 102–106.
Ketcham, W. M., and P. V. Hobbs (1969), An experimental determination of the surface energies of ice, *Philos. Mag. A.*, *19*, 1161–1173.
Kirchner, H. O. K., G. Michot, and T. Suzuki (2000), Fracture toughness of snow in tension, *Philos. Mag. A*, *80*(5), 1265–1272.
Kirchner, H. O. K., G. Michot, and J. Schweizer (2002a), Fracture toughness of snow in shear and tension, *Scr. Mater.*, *46*, 425–429.
Kirchner, H. O. K., G. Michot, and J. Schweizer (2002b), Fracture toughness of snow in shear under friction, *Phys. Rev. E.*, *66*(2), 027103.
Kirchner, H. O. K., H. Peterlik, and G. Michot (2004), Size independence of the strength of snow, *Phys. Rev. E.*, *69*(1), 011306.
Kojima, K. (1954), Visco-elastic properties of snow layers, *Low Temp. Sci., Ser. A*, *12*, 1–13, (In Japanese with English summary).
Kronholm, K. (2004), Spatial variability of snow mechanical properties, Ph.D. thesis, 187 pp., Fac. of Nat. Sci. and Eng., Eidg. Tech. Hochsch., Zürich, Switz.
Kronholm, K., and J. Schweizer (2003), Snow stability variation on small slopes, *Cold Reg. Sci. Technol.*, *37*, 453–465.
Landry, C., K. W. Birkeland, K. Hansen, J. J. Borkowski, R. L. Brown, and R. Aspinall (2004), Variations in snow strength and stability on uniform slopes, *Cold Reg. Sci. Technol.*, *39*, 205–218.
McCammon, I., and J. Schweizer (2002), A field method for identifying structural weaknesses in the snowpack, in *Proceedings of the International Snow Science Workshop, 2002: Penticton, B. C.*, edited by J. R. Stevens, pp. 477–481, Int. Snow Sci. Workshop Canada Inc., Penticton, B. C., Canada.
McClung, D. M. (1977), Direct simple shear tests on snow and their relation to slab avalanche formation, *J. Glaciol.*, *19*(81), 101–109.
McClung, D. M. (1979), Shear fracture precipitated by strain-softening as a mechanism of dry slab avalanche release, *J. Geophys. Res.*, *84*(B7), 3519–3526.
McClung, D. M. (1981), Fracture mechanical models of dry slab avalanche release, *J. Geophys. Res.*, *86*(B11), 10,783–10,790.
McClung, D. M. (2003), Size scaling for dry snow slab release, *J. Geophys. Res.*, *108*(B10), 2465, doi:10.1029/2002JB002298.
McClung, D. M. (2005a), Dry slab avalanche shear fracture properties from field measurements, *J. Geophys. Res.*, *110*, F04005, doi:10.1029/2005JF000291.
McClung, D. M. (2005b), Approximate estimates of fracture speeds for dry slab avalanches, *Geophys. Res. Lett.*, *32*(8), L08406, doi:10.1029/2005GL022391.
McClung, D., and P. Schaerer (1993), *The Avalanche Handbook*, 271 pp., Mountaineers, Seattle.
McClung, D. M., and J. Schweizer (1999), Skier triggering, snow temperatures and the stability index for dry-slab avalanche initiation, *J. Glaciol.*, *45*(150), 190–200.
Mellor, M. (1975), A review of basic snow mechanics, in *Proceedings of the Grindewald Symposium, Switzerland, April, 1974*, *IAHS-Publ. 114*, 251–291.
Narita, H. (1980), Mechanical behaviour and structure of snow under uniaxial tensile stress, *J. Glaciol.*, *26*(94), 275–282.
Narita, H. (1983), An experimental study on tensile fracture of snow, *Contrib. Inst. Low Temp. Sci., Ser. A*, *32*, 1–37.
Nixon, W. A., and E. M. Schulson (1987), A micromechanical view of the fracture toughness of ice, *J. Phys. Colloq.*, *C1*(48), 313–320.
Palmer, A. C., and J. R. Rice (1973), The growth of slip surfaces in the progressive failure of over-consolidated clay, *Proc. R. Soc. London, Ser. A*, *332*, 527–548.
Perla, R. (1971), The Slab Avalanche, 100 pp., Ph.D. thesis, Dept. of Meteorol., U. of Utah, Salt Lake City, Utah.
Perla, R. (1977), Slab avalanche measurements, *Can. Geotech. J.*, *14*(2), 206–213.
Petrenko, V. F., and R. W. Whitworth (1999), *Physics of Ice*, 373 pp. Oxford Univ. Press, New York.
Rice, J. R. (1968), Mathematical analysis in the mechanics of fracture, in *Fracture: An Advanced Treatise*, volume 2, *Mathematical Fundamentals*, edited by H. Liebowitz, pp. 192–311, Elsevier, New York.

Schweizer, J., and J. B. Jamieson (2001), Snow cover properties for skier triggering of avalanches, *Cold Reg. Sci. Technol.*, *33*, 207–221.
Schweizer, J., G. Michot, and H. O. K. Kirchner (2004), On the fracture toughness of snow, *Ann. Glaciol.*, *38*, 1–8.
Sigrist, C., J. Schweizer, H. J. Schindler, and J. Dual (2005), On size and shape effects in snow fracture toughness measurements, *Cold Regions Science and Technology*, *43*, 24–35.
Sommerfeld, R. A. (1974), A Weibull prediction of the tensile strength-volume relationship of snow, *J. Geophys. Res.*, *79*(23), 3353–3356.
Sommerfeld, R. A. (1980), Statistical models of snow strength, *J. Glaciol.*, *26*(94), 217–223.
Stethem, C., and R. Perla (1980), Snow-slab studies at Whistler Mountain, British Columbia, Canada, *J. Glaciol.*, *26*(94), 85–91.
Weibull, W. (1939), A statistical theory of the strength of materials, *Proc. R. Swed. Acad. Eng. Sci.*, *151*, 1–45.
Weibull, W. (1951), A statistical distribution function of wide applicability, *J. Appl. Mech.*, *18*, 293–297.

D. M. McClung, Department of Geography, University of British Columbia, Vancouver, BC, V6T 1Z2 Canada. (mcclung@geog.ubc.ca)
J. Schweizer, WSL, Swiss Federal Institute for Snow and Avalanche Research, Flüelastrasse 11, CH-7260 Davos, Switzerland.